

Quantum memory and non-demolition measurement of single phonon state with nitrogen-vacancy centers ensemble

Rui-xia Wang,¹ Kang Cai,¹ Zhang-qi Yin,^{2,*} and Gui-lu Long^{1,†}

¹*Department of Physics, Tsinghua University, Beijing 100084, China*

²*Center for Quantum Information, Institute for Interdisciplinary Information Sciences, Tsinghua University, Beijing 100084, China*

(Dated: October 9, 2018)

In diamond, the mechanical vibration induced strain can lead to interaction between the mechanical mode and the nitrogen-vacancy (NV) centers. In this work, we propose to utilize the strain induced coupling for the quantum non-demolition (QND) single phonon measurement and memory in diamond. The single phonon in a diamond mechanical resonator can be perfectly absorbed and emitted by the NV centers ensemble (NVE) with adiabatically tuning the microwave driving. An optical laser drives the NVE to the excited states, which have much larger coupling strength to the mechanical mode. By adiabatically eliminating the excited states under large detuning limit, the effective coupling between the mechanical mode and the NVE can be used for QND measurement of the single phonon state. Under realistic experimental conditions, we numerically simulate the scheme. It is found that the fidelity of the absorbing and emitting process can reach a much high value. The overlap between the input and the output phonon shapes can reach 98.57%.

PACS numbers: 63.20.kp, 63.20.dd, 03.67.Lx

I. INTRODUCTION

In quantum information processing, one of the key challenges is to realize the effective coupling, or communication, between distant qubits. Usually, the photon is used as flying qubit for quantum communications [1], or inducing the effective coupling between the distant qubits [2]. For example, in superconducting quantum circuit systems, the microwave photon confined in transmission lines resonator is used as a quantum bus [3]. Recently, with the advances in the fabrication and manipulation of the mechanical systems [4–7], an alternative way of using phonon to couple distant qubits was proposed [8]. The surface acoustic wave (SAW) has been successfully coupled with superconducting qubits [9, 10]. The advantages of the phonon quantum bus compared with the photon quantum bus are the high quality factor and small effective size [8, 9, 11]. The speed of SAW is 5 orders of magnitude slower than the speed of light [10, 12]. Therefore, the wavelength of SAW at GHz is also 5 orders of magnitude smaller than the microwave light. In this way, the individual superconducting qubit addressing by SAW is possible. There are many schemes concerning single phonons, for example, the phonon states preparation [13–15], detection [13–20], and the phonon mediated interface [21].

As we know, in quantum optics experiments, the single photon detectors are widely used. For microwave photons, the quantum non-demolish (QND) measurement for photon number states has been realized in both cavity QED and superconducting circuit QED systems [22].

The QND measurement in circuit QED systems can be used for quantum error corrections. In order to further develop the phonon based quantum information processing, the efficient single phonon detector is needed. The ultimate goal is to realize QND measurement on single phonon state. Inspired by the QND measurement for photon number states, we use the strain induced phonon and the NVE coupling in the diamond to get the strong nonlinearity for the QND measurement of the single phonon state. The geometry of the mechanical crystal structure contains a diamond crystal with rectangular holes arranged periodically which can precisely manipulate mechanical vibrations [23].

The nitrogen-vacancy (NV) center, which consists a substitutional nitrogen atom and adjacent vacancy in diamond, is one of the most promising system for solid-state quantum information processing. NV centers can be controlled by microwave with long coherence time even at room temperature. The diamond lattice vibration, or phonon, can couple with the NV centers ensemble (NVE) [24, 25] and be cooled by the NVE [26]. There are two different kind of mechanism for coupling the NV center and the phonons. The first one is magnetic field induced coupling [27–33], and the second one is the strain induced coupling [34–36]. Here we focus on the second method. The strain induced coupling between NV centers electron spins in the ground state and the phonons is usually quite small, e.g. less than 1 kHz [34]. Recently, the excited-state electron-phonon coupling has been reported in experiments [36]. It is about 6 orders of magnitude stronger than the ground-state electron-phonon coupling [37, 38]. By taking the advantage of strong coupling, the quantum control of the internal states of a NV center has been realized by using optomechanical sideband transition [36]. We can use this strong coupling mechanism to induce the strong effective nonlinear coupling between the phonon

* yinzhangqi@tsinghua.edu.cn

† gllong@tsinghua.edu.cn

and the NVE, and realized QND phonon number measurement.

In this work, the strain-induced spin-phonon coupling is employed in designing the scheme for the single phonon absorption, emission and QND measurement. We consider the NVE situated a few μm below the diamond surface which is shown in Fig. 1(a). The coupling strength between the NVE and the single phonon can be enhanced by a factor \sqrt{N} through the collective excitation, which can reach the strong coupling regime. The resonant frequency of the phonons propagating in the diamond can be controlled by the rectangular holes shown in the upper diagram of Fig. 1(a), which are periodically arranged on the diamond chip. The single phonon with the resonant frequency can be absorbed by the NVE, and the absorption will induce the resonant frequency shift which can be revealed in the phonon absorption spectrum, then we can detect the single phonon state through probing the resonance frequency shift of the phonons in the diamond.

The inverse process of the single phonon detection is a emission process. The emitted phonon shape can be controlled by regulating the driving pulse acting on the NVE. The similarity between the emitted and the absorbed single phonon reaches 98.57% if we inverse the driving pulse when emitting compared with the absorbing process. If the single phonon state is in quantum state before absorbing, the size and shape of the phonon will not be changed when emitting, this process is a quantum non-demolition (QND) measurement process, which realizes an ideal projective measurement that leaves the system in an eigenstate of the phonon number [22, 39–41].

II. MODEL

As schematically shown in Fig. 1(a), we consider a diamond chip with periodically arranged rectangle holes to adjust the refractive index for the surface acoustic wave (SAW). The NVE are located near the diamond surface coupling to the laser, microwave and SAW.

With a zero magnetic field, the spin-triplet ground state of the NV center splits into two energy levels, $M_s = 0$ and the nearly degenerate sublevels $M_s = \pm 1$ [42]. We apply an external magnetic field \vec{B}_{ext} along the crystalline direction [100] of the NV center [43] to split the degenerate sublevels $M_s = \pm 1$, which results in a three-level system denoted by $|0\rangle = |^3A, M_s = 0\rangle$, $|-1\rangle = |^3A, M_s = -1\rangle$, $|+1\rangle = |^3A, M_s = +1\rangle$, respectively. $|E\rangle$ is an excited state with an energy gap of about 1.189eV to the ground state.[44] The schematic diagram of the NV center energy structure is shown in Fig. 1(b).

The NV centers exist in a diamond crystal and they can sense the lattice vibrations. If there is a phonon produced in the lattice, the NV center can absorb it when the mechanical frequency and the energy splitting of the NV centers are matched [34, 45]. For this system, the phonon mode a_m with the frequency ω_m couples to the

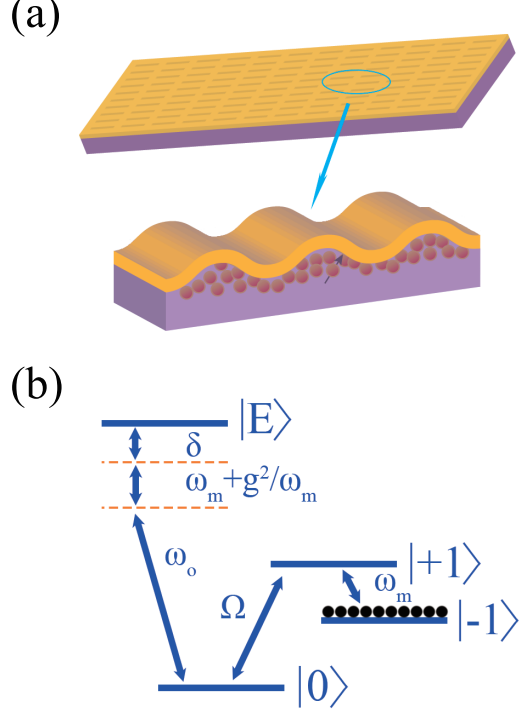


FIG. 1. (a) A schematic diagram of the phononic crystal. The NVE located near the surface coupling to a single phonon and a laser field. (b) The electronic structure of the NV center. Ω is the Rabi frequency between the energy levels $|0\rangle$ and $|+1\rangle$ induced by the microwave drive. ω_m is the phonon mode. ω_0 is the optical driving frequency between the energy levels $|0\rangle$ and $|E\rangle$ inducing the Rabi frequency of Ω_0 .

NV centers with transition of $|-1\rangle$ to $|+1\rangle$. A classical microwave field $\varepsilon(t) = \tilde{\varepsilon}(t) e^{-i\omega_{01}t}$ drives the transition $|+1\rangle$ to $|0\rangle$ with a Rabi oscillation frequency $\Omega(t)$ (ω_{01} is the frequency splitting between the levels $|0\rangle$ and $|+1\rangle$). The Rabi frequency $\Omega(t)$ can be written as $\Omega(t) = \Omega_0 \alpha(t)$. Within a good approximation, we assume that $\tilde{\varepsilon}(t)$ increase gradually from zero with $\tilde{\varepsilon}(0) \simeq 0$ to a finite strength. Because $\alpha(t)$ is proportional to $\tilde{\varepsilon}(t)$ ($\alpha(t) \propto \tilde{\varepsilon}(t)$), then we can get $\Omega(t) = \Omega'_0 \tilde{\varepsilon}(t)$, which describes that the shape of the amplitude of the classical driving microwave field totally decides the Rabi frequency.

Neglecting the dissipation of the NVE system, the Hamiltonian of the NVE system including the coupling between the mode a_m and the output can be written as

(setting $\hbar = 1$) [46, 47]

$$\begin{aligned}
H = & \sum_{i=1}^N G_m (|+1\rangle_i \langle -1| a_m + |-1\rangle_i \langle +1| a_m^\dagger) \\
& + \frac{\Omega(t)}{2} \sum_{i=1}^N (|0\rangle_i \langle +1| + |+1\rangle_i \langle 0|) \\
& + i\sqrt{\kappa/2\pi} \int_{+\Delta\omega_e}^{+\Delta\omega_e} d\omega [a_m^\dagger e(\omega) - a_m e^\dagger(\omega)] \\
& + \int_{+\Delta\omega_e}^{+\Delta\omega_e} d\omega [\omega e^\dagger(\omega) e(\omega)]. \quad (1)
\end{aligned}$$

Where G_m is the coupling rate between single NV center and the phonon, which is typically small. $e(\omega)$ denotes the one-dimensional phonon modes which are free in the diamond and couple to the phonon mode a_m . We need to consider the free propagating modes within a finite bandwidth $[\omega_e - \Delta\omega_e, \omega_e + \Delta\omega_e]$ that couple to the NV mode with the carrier frequency ω_e . Within this bandwidth, the coupling between $e(\omega)$ and the NV is a constant approximately which is denoted by $\sqrt{\kappa/2\pi}$ for convenience. κ is the effective decay rate.

To obtain the relationship between the driving pulse shape and the output phonon pulse shape, a simple picture by neglecting the dissipation of the NVE system and the coupling of the mode a_m to the output is studied. Initially, the NVE are cooled to the ground state $|0\rangle$, and a π pulse is driven between the state $|0\rangle$ and $|-1\rangle$, and then the NVE is in $|-1\rangle^{\otimes N}$. We assume that the phonon mode frequency ω_m equals to ω_e (ω_e is the frequency splitting between the levels $|-1\rangle$ and $|+1\rangle$). In the rotating frame, the Hamiltonian of the NVE system is

$$\begin{aligned}
H' = & \sum_{i=1}^N G_m (|+1\rangle_i \langle -1| a_m + |-1\rangle_i \langle +1| a_m^\dagger) \\
& + \frac{\Omega(t)}{2} \sum_{i=1}^N (|0\rangle_i \langle +1| + |+1\rangle_i \langle 0|). \quad (2)
\end{aligned}$$

We map the operator $|+1\rangle_i \langle -1|$ to the bosonic operators. $\sqrt{N}a^\dagger = \sum_{i=1}^N |+1\rangle_i \langle -1|$, $a^\dagger a|n\rangle_{+1} = n|n\rangle_{+1}$ means there are n NVs that are in the state $|+1\rangle$. $d^\dagger = |0\rangle_i \langle +1|$ and $d = |+1\rangle_i \langle 0|$ are the creation and annihilation operators for the i th NV center, and then the Hamiltonian can be written as follow, where $g_m = \sqrt{N}G_m$.

$$H' = g_m(a^\dagger a_m + a a_m^\dagger) + \frac{\Omega(t)}{2}(d^\dagger + d). \quad (3)$$

In the bases of $|N\rangle_{-1}|0\rangle_{+1}|0\rangle_0|1\rangle_m$, $|N-1\rangle_{-1}|1\rangle_{+1}|0\rangle_0|0\rangle_m$, $|N-1\rangle_{-1}|0\rangle_{+1}|1\rangle_0|0\rangle_m$, where the state $|p\rangle_{-1}|q\rangle_{+1}|r\rangle_0|s\rangle_m$ represents that the numbers of the NVs which are in the states $|-1\rangle$, $|+1\rangle$, and $|0\rangle$ are p , q and r respectively, and the number of phonons in the diamond is s . The Hamiltonian can be written as

a matrix as follow in the three bases,

$$H' = \begin{bmatrix} 0 & g_m & 0 \\ g_m & 0 & \frac{\Omega(t)}{2} \\ 0 & \frac{\Omega(t)}{2} & 0 \end{bmatrix}. \quad (4)$$

This Hamiltonian has the well-known dark state $|D\rangle$ with the form $|D\rangle = \frac{-\Omega(t)/2}{\sqrt{g_m^2 + [\Omega(t)/2]^2}} |N\rangle_{-1}|0\rangle_{+1}|0\rangle_0|1\rangle_m + \frac{g_m}{\sqrt{g_m^2 + [\Omega(t)/2]^2}} |N-1\rangle_{-1}|0\rangle_{+1}|1\rangle_0|0\rangle_m$. The dark state means, the state will remain on the state $|D\rangle$, if the driving pulse $\Omega(t)$ and the coupling strength satisfy the relationship $\cos\theta = \frac{\Omega(t)/2}{\sqrt{g_m^2 + [\Omega(t)/2]^2}}$ and $\sin\theta = \frac{g_m}{\sqrt{g_m^2 + [\Omega(t)/2]^2}}$.

The effects of non-zero dissipation will be analyzed in section IV where the phonon detecting efficiency is calculated as well as the overlap of the absorbing and emitting a single phonon with the real lossy system.

III. PULSE SHAPE

To obtain the relationship of the pulse shape between the driving and the phonon, we first consider the emitting process from state $|N-1\rangle_{-1}|0\rangle_{+1}|1\rangle_0|0\rangle_m$ to $|N\rangle_{-1}|0\rangle_{+1}|0\rangle_0|1\rangle_m$ under ideal conditions. The Hamiltonian of the system can be written as

$$\begin{aligned}
H = & g_m (a^\dagger a_m + a a_m^\dagger) + \frac{\Omega(t)}{2}(d^\dagger + d) \\
& + i\sqrt{\kappa/2\pi} \int_{-\Delta\omega_e}^{+\Delta\omega_e} d\omega [a_m^\dagger e(\omega) - a_m e^\dagger(\omega)] \\
& + \int_{-\Delta\omega_e}^{+\Delta\omega_e} d\omega [\omega e^\dagger(\omega) e(\omega)]. \quad (5)
\end{aligned}$$

Assume that, at the time $t = 0$, the Rabi frequency $\Omega(t) = 0$, the NVE system are in the state $|N-1\rangle_{-1}|0\rangle_{+1}|1\rangle_0|0\rangle_m$, after applying a classical driving pulse $\varepsilon(t)$, the Rabi frequency, which is proportional to the intensity of the driving pulse, changes slowly and is within the adiabatic approximation. Then we can expand the state $|\Psi\rangle$ of the whole system into the following form [46]

$$|\Psi\rangle = c_d |D\rangle \otimes |\phi_0\rangle + |N\rangle_{-1}|0\rangle_{+1}|0\rangle_0|0\rangle_m \otimes |\phi_1\rangle, \quad (6)$$

where $|\phi_0\rangle$ denotes the vacuum state of mode $e(\omega)$ in the diamond, and

$$|\phi_1\rangle = \int_{-\Delta\omega_e}^{+\Delta\omega_e} d\omega c_\omega e^\dagger(\omega) |\phi_0\rangle, \quad (7)$$

represents the single phonon output state. Initially, $c_d = 1$, $c_\omega = 0$ and $\Omega(0) = 0$. Within the adiabatic approximation, we would like to calculate the time evolution of the whole NVE system state $|\Psi\rangle$ by substituting it into the schrödinger equation $i\partial_t|\Psi\rangle = H|\Psi\rangle$. The coefficients c_d and c_ω can be got, which satisfy the following

evolution equations:

$$\dot{c}_d = \left(-\sqrt{\kappa/2\pi} \cos \theta \right) \int_{-\Delta\omega_e}^{+\Delta\omega_e} c_\omega d\omega, \quad (8)$$

$$\dot{c}_\omega = -i\omega c_\omega + \sqrt{\kappa/2\pi} c_d \cos \theta. \quad (9)$$

We can get the solution of c_ω as follow

$$c_\omega(t) = \sqrt{\kappa/2\pi} \int_0^t e^{-i\omega(t-\tau)} c_d(\tau) \cos \theta(\tau) d\tau, \quad (10)$$

substituting the solution into the equation of c_d , leads to

$$\dot{c}_d = -\frac{\kappa \cos \theta}{\pi} \int_0^t \frac{\sin[\delta\omega(t-\tau)]}{(t-\tau)} c_d(\tau) \cos \theta(\tau) d\tau \quad (11)$$

The bandwidth $\delta\omega$ satisfies $\delta\omega T \gg 1$, where the operation time T characterizes the time scale for a significant change of c_d and $\sin \theta$, so the above function satisfies a δ function

$$\delta(x) = \lim_{k \rightarrow \infty} \frac{1}{\pi} \frac{\sin kx}{x}, \quad (12)$$

then we can obtain

$$\dot{c}_d = -\frac{\kappa}{2} c_d(t) \cos^2 \theta, \quad (13)$$

The solution of c_d and c_ω are

$$c_d = e^{-\frac{\kappa}{2} \int_0^t \cos^2 \theta(\tau) d\tau}, \quad (14)$$

$$c_\omega(t) = \sqrt{\kappa/2\pi} \int_0^t e^{-i\omega(t-\tau)} e^{-\frac{\kappa}{2} \int_0^t \cos^2 \theta(\tau) d\tau} \cdot \cos \theta(\tau) d\tau. \quad (15)$$

The single-phonon pulse shape $f(t)$ can be obtained by the Fourier transformation

$$f(t) = \frac{1}{\sqrt{2\pi}} \int_{-\Delta\omega_e}^{+\Delta\omega_e} d\omega c_\omega(T) e^{-i\omega(t-T)} \quad (16)$$

$$= \sqrt{\kappa} \cos \theta(t) e^{-\frac{\kappa}{2} \int_0^t \cos^2 \theta(\tau) d\tau}. \quad (17)$$

If the Rabi frequency $\Omega(t)$, which is proportional to the strength of the driving pulse, satisfies the function as $\Omega(t) = 2g_m \exp[\kappa(t - \frac{T}{2})/2]$, the output phonon shape will be symmetric. The output phonon shape function can be figured out as

$$f(t) = \frac{\sqrt{\kappa} \sqrt{1 + \exp(-\frac{\kappa T}{2})}}{\exp[-\kappa(t - \frac{T}{2})/2] + \exp[\kappa(t - \frac{T}{2})/2]}, \quad (18)$$

the results is shown in Fig. 3 for $\kappa/2\pi = 1.6 \times 10^5$, $T = \frac{20}{\kappa}$. We assume that, in the absorption process, we know the phonon shape in advance, such as the shape in Fig. 2. As the absorption process is the time reversal of the emission process, and the phonon shape is symmetrical in the time domain, if we reverse the temporal driving pulse shape on NV centers in the absorbing process, the phonon can be completely absorbed by the NVE [48]. If the phonon shape is not symmetrical in the time domain, it can also be completely absorbed as long as it is reversed simultaneously with the driving pulse.

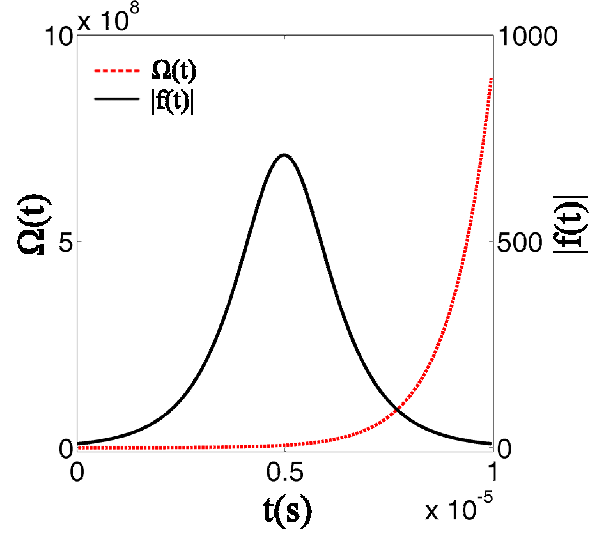


FIG. 2. The situation of the symmetric output phonon shape. The red line is the driving pulse shape applying to the NVE, and the black line represents the pulse shape of the output phonon.

IV. QND MEASUREMENT

As schematically shown in Fig. 1, we consider the energy levels $|0\rangle$ and $|E\rangle$. After the absorption process, we stop the driving pulse Ω between the state $|0\rangle$ and $|+1\rangle$ and start the driving pulse Ω_o between the state $|0\rangle$ and $|E\rangle$ to detect the single phonon state.

The Hamiltonian of the detecting system is

$$H = \omega_m a_m^\dagger a_m + \omega_{0E} |E\rangle \langle E| + \frac{\Omega_o}{2} (e^{i\omega_o t} |0\rangle \langle E| + e^{-i\omega_o t} |E\rangle \langle 0|) + g(a_m^\dagger + a_m) |E\rangle \langle E| \quad (19)$$

Applying the Schrieffer-Wolff transformation

$$U = \exp\left[\frac{g}{\omega_m} (a_m^\dagger - a_m) |E\rangle \langle E|\right]$$

to the Hamiltonian gives

$$\begin{aligned} \tilde{H} &= U H U^\dagger \\ &= \omega_m a_m^\dagger a_m - \frac{g^2}{\omega_m} |E\rangle \langle E| + \omega_{0E} |E\rangle \langle E| \\ &\quad + \frac{\Omega_o}{2} [e^{i\omega_o t - \frac{g}{\omega_m}(a_m^\dagger - a_m)} |0\rangle \langle E| + H.c.] \end{aligned} \quad (20)$$

Apply the RWA, and set $H_0 = \omega_m a_m^\dagger a_m + (\omega_{0E} - \frac{g^2}{\omega_m} - \delta) |E\rangle \langle E|$, the Hamiltonian becomes

$$\tilde{H}_r = \delta |E\rangle \langle E| + \frac{g\Omega_o}{2\omega_m} a_m^\dagger |E\rangle \langle 0| + \frac{g\Omega_o}{2\omega_m} a_m |0\rangle \langle E| \quad (21)$$

Where $\omega_{0E} = \delta + \omega_m + \frac{g^2}{\omega_m} + \omega_o$.

Then we apply another RWA, and set $H'_0 = \delta|E\rangle\langle E|$, the Hamiltonian is calculated as

$$\tilde{H}'_r = \frac{g\Omega_o}{2\omega_m} e^{i\delta t} a_m^\dagger |E\rangle\langle 0| + \frac{g\Omega_o}{2\omega_m} e^{-i\delta t} a_m |0\rangle\langle E| \quad (22)$$

When the interaction strength of $\frac{\Omega_o}{2}$ is far small compared with the detuning δ , the time-average effective Hamiltonian is obtained as [49]

$$\begin{aligned} \tilde{H}'_{eff} = & \frac{g^2\Omega_o^2}{4\omega_m^2\delta} a_m^\dagger a_m (|E\rangle\langle E| - |0\rangle\langle 0|) \\ & - \frac{g^2\Omega_o^2}{4\omega_m^2\delta} |0\rangle\langle 0| \end{aligned} \quad (23)$$

From the Hamiltonian we can see that the resonant frequency of the phonon crystal will be affected by the state of NVE, which means the resonant frequency shift is proportional to the excitation number in state $|0\rangle$. When there is one NV center absorbing a single phonon, the frequency shift of the phonon crystal is

$$\Delta f_s = \frac{g^2\Omega_o^2}{2\omega_m^2\delta}. \quad (24)$$

The effective dissipation of the excited state $|E\rangle$ is $\gamma_e = (\frac{\bar{g}}{\delta})^2 \gamma_E$, where $\bar{g} = \frac{g\Omega_o}{2\omega_m}$ is the equivalent coupling strength, γ_E is the decay rate of the energy level $|E\rangle$ with the population of 1. If we set $g = 2\pi \times 5 MHz$, $\Omega_o = 2\pi \times 290 MHz$, $\omega_m = 2\pi \times 900 MHz$ [36], $\gamma_E = 2\pi \times 3 MHz$ [50], and $\delta = 2\pi \times 30 MHz$, the effective dissipation and the frequency shift can be calculated as $\gamma_e = 2\pi \times 2.16 kHz$ and $\Delta f_s = 2\pi \times 43.26 kHz$ respectively, which implies that the single phonon absorption induced frequency shift can be detected distinctively. In fact, as long as we have $\delta \gg \gamma_E$, the demand for the resolution can be satisfied, and the scheme can be realized under the realistic experimental conditions.

V. DISSIPATION EFFECTS

In the above sections, the dynamical evolution has been analysed in ideal condition and the relationship between the driving pulse shape and the emitting phonon shape has been obtained, however, there are various losses in the real systems. If we consider the dynamical evolution of the NVE system with the conditional Hamiltonian which include the possible losses, the whole conditional Hamiltonian has the following form:

$$\begin{aligned} H_c = & -i\frac{\gamma_1}{2} |N-1\rangle_{-1} |1\rangle_{+1} |0\rangle_0 |0\rangle_m \\ & -i\frac{\gamma_0}{2} |N-1\rangle_{-1} |0\rangle_{+1} |1\rangle_0 |0\rangle_m - i\frac{\gamma_m}{2} a_m^\dagger a_m \\ & + g_m (a^\dagger a_m + a a_m^\dagger) + \frac{\Omega(t)}{2} (d^\dagger + d) \\ & + i\sqrt{\kappa/2\pi} \int_{-\Delta\omega_e}^{+\Delta\omega_e} d\omega [a_m^\dagger e(\omega) - a_m e^\dagger(\omega)] \\ & + \int_{-\Delta\omega_e}^{+\Delta\omega_e} d\omega [\omega e^\dagger(\omega) e(\omega)]. \end{aligned} \quad (25)$$

Where γ_0 is the dephasing rate in state $|0\rangle$, γ_1 denotes the spontaneous emission of state $|+1\rangle$, and γ_m denotes the phonon dissipation in the single NV evolution.

For numerical simulations, we need to discretize the field $e(\omega)$ by introducing a finite but small frequency interval $\delta\omega$ between two adjacent mode frequency. Then the number of the total modes we have is $n = \frac{2\Delta\omega_e}{\delta\omega} + 1$, the frequency of the j th mode ω_j which is denoted by e_j is given by $\omega_j = (j - \frac{n+1}{2}) \delta\omega$. The Hamiltonian can be transformed to the form:

$$\begin{aligned} H_c = & -i\frac{\gamma_1}{2} |N-1\rangle_{-1} |1\rangle_{+1} |0\rangle_0 |0\rangle_m \\ & -i\frac{\gamma_0}{2} |N-1\rangle_{-1} |0\rangle_{+1} |1\rangle_0 |0\rangle_m - i\frac{\gamma_m}{2} a_m^\dagger a_m \\ & + g_m (a^\dagger a_m + a a_m^\dagger) + \frac{\Omega(t)}{2} (d^\dagger + d) \\ & + i\kappa_e \sum_{j=1}^n \sqrt{\delta\omega} [a_m^\dagger e_j - a_m e_j^\dagger] \\ & + \sum_{j=1}^n (\omega_j \delta\omega e_j^\dagger e_j), \end{aligned} \quad (26)$$

where $\kappa_e = \sqrt{\kappa\delta\omega/2\pi}$. Similarly, the state $|\Psi\rangle$ of the NVE system can be expanded by the discretized phonon pulse state with the form $|\phi_1\rangle = \sum_{j=1}^n \delta\omega b_j e_j^\dagger |vac\rangle$, which is

$$\begin{aligned} |\Psi\rangle = & (c_1 |N\rangle_{-1} |0\rangle_{+1} |0\rangle_0 |1\rangle_m + c_2 |N-1\rangle_{-1} |1\rangle_{+1} |0\rangle_0 |0\rangle_m \\ & + c_3 |N-1\rangle_{-1} |0\rangle_{+1} |1\rangle_0 |0\rangle_m) \otimes |\phi_0\rangle \\ & + |N\rangle_{-1} |0\rangle_{+1} |0\rangle_0 |0\rangle_m \otimes |\phi_1\rangle. \end{aligned} \quad (27)$$

Substituting $|\Psi\rangle$ into the schrödinger equation $i\partial_t |\Psi\rangle = H|\Psi\rangle$, we can get

$$\dot{c}_1 = -\frac{\gamma_m}{2} c_1 - i g_m c_2 + \kappa_e \sum_{j=1}^n \tilde{b}_j, \quad (28)$$

$$\dot{c}_2 = -\frac{\gamma_1}{2} c_2 - i g_m c_1 - i\frac{\Omega(t)}{2} c_3, \quad (29)$$

$$\dot{c}_3 = -\frac{\gamma_0}{2} c_3 - i\frac{\Omega(t)}{2} c_2, \quad (30)$$

$$\dot{b}_j = -\kappa_e c_1 - i\tilde{b}_j \omega_j, \quad (31)$$

where $\tilde{b}_j = \sqrt{\delta\omega} b_j$. We assume that, initially, there is a single phonon state in the diamond, which shape is shown as Fig. 2, and all of the NV centers are in the state $|-1\rangle$, which means $c_1 = c_2 = c_3 = 0$, $\sum |b_j|^2 \neq 0$. If we would like to absorb the phonon effectively, the driving pulse $\Omega'(t)$ should be the time reversal of $\Omega(t)$ in Fig. 2, that is $\Omega'(t) = g_m \exp[\kappa(-t + \frac{T}{2})/2]$, where $T = 20/\kappa$. The shape control of the driving microwave pulse can be easily achieved by modulating an arbitrary wave generator. We set $\gamma_0/2\pi = 0.16 kHz$, $\gamma_1/2\pi = 0.16 kHz$ [51], $\gamma_m/2\pi = 0.16 kHz$ [24, 52], $g_m/2\pi = 0.96 MHz$,

and $\kappa/2\pi = 0.32\text{MHz}$. The numerical simulation results of absorbing process is shown in Fig. 3a with the black lines. Under the condition of strong coupling between the NVE and the phonon, the process is quasi-adiabatic, the value of c_2 is distinctly smaller than c_1 and c_3 . The first half is the process that the free single phonon entering the strong coupling area with the NVE plays a leading role, and the later half is predominantly the absorbing process. at time $t = T$, the fidelity between the actual state and the ideal state is 99.38%. As the dissipations increase, the fidelity decreases obviously which is also shown in Fig. 3a with the blue lines. The red lines in Fig. 3a implies that, it will also reduce the fidelity of the state if the coupling strength and the effective decay rate κ do not satisfy the adiabatic condition.

After absorbing and detecting the single phonon, we can apply a driving pulse $\Omega(t)$ on the NVE, the phonon we have just absorbed will then be emitted. The comparison of the input and output phonon pulse shape is shown in Fig. 3b with the $\kappa = 0.32\text{MHz}$. The black line is the input phonon shape, the red, blue and green ones are the output phonon shape with $g_m/2\pi = 0.96\text{MHz}$, 0.64MHz and 0.32MHz respectively. we can see that, the more stronger the coupling is, the larger overlap it has between the input and output single phonon shape. When the coupling strength $g_m/2\pi = 0.96\text{MHz}$, the overlap can reach 98.57. In the first step, the NVE absorbs one phonon from the diamond or not. And then, we can detecting whether the single phonon state was absorbed through the frequency shift of the phononic crystal. Finally, the NVE can emit the phonon with nearly the same shape compared with the absorbed one. In this process, the single phonon state has been measured without changing the phonon shape, which is a true QND measurement. The process of emitting can act as a single phonon source. The whole courses including absorbing, detecting and emitting a single phonon can also serve as a single phonon memory.

VI. CONCLUSION

We have proposed a scheme to realize the QND single phonon state detecting and emitting based on the strain mediated interaction between the NVE and the single phonon. By analyze the dynamical evolution of the real system, we are able to calculate the fidelity of the absorbing process and the overlap between the input and output phonon number state, both of which can reach a very high value. The emitting process can act as a single phonon source and the whole courses including absorbing, detecting and emitting a single phonon can also serve as a single phonon memory. In future, the similar method may also be used to realize the QND measurement for arbitrary Fock states of phonons.

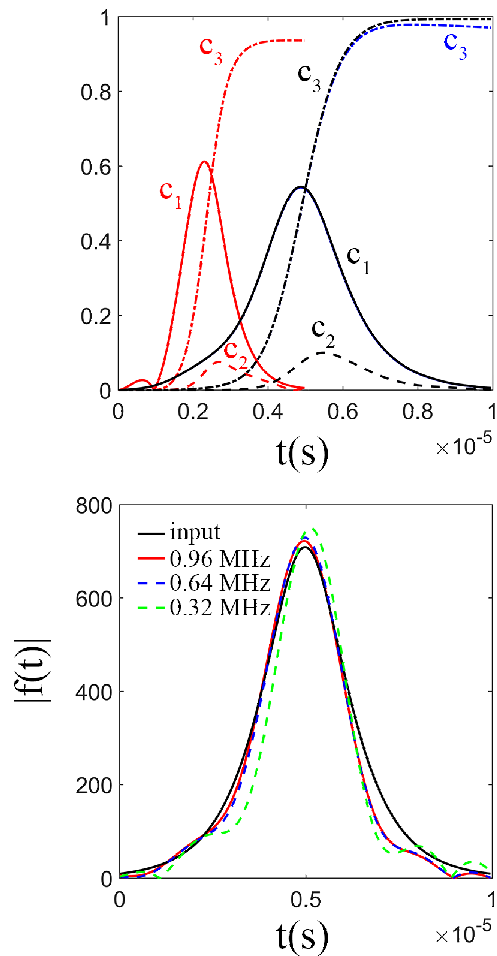


FIG. 3. The numerical simulation results. (a) is the absorbing process. The black lines represents the process with $\gamma_0/2\pi = 0.16\text{kHz}$, $\gamma_1/2\pi = 0.16\text{kHz}$, $\gamma_m/2\pi = 0.16\text{kHz}$, $g_m/2\pi = 0.96\text{MHz}$, and $\kappa/2\pi = 0.32\text{MHz}$. The blue lines show the process with $\gamma_0/2\pi = 1.6\text{kHz}$, $\gamma_1/2\pi = 1.6\text{kHz}$, $\gamma_m/2\pi = 1.6\text{kHz}$, $g_m/2\pi = 0.96\text{MHz}$, and $\kappa/2\pi = 0.32\text{MHz}$. The red ones denote the process with $\gamma_0/2\pi = 0.16\text{kHz}$, $\gamma_1/2\pi = 0.16\text{kHz}$, $\gamma_m/2\pi = 1.92\text{MHz}$, and $\kappa/2\pi = 0.64\text{MHz}$. (b) is the emitting process, where the black line represents the input phonon shape, and the red, blue and green lines represent the output phonon shapes when the coupling strength are at $g_m/2\pi = 0.96\text{MHz}$, 0.64MHz and 0.32MHz respectively with the same value of $\kappa = 0.32\text{MHz}$. The overlap between the input pulse and the output pulse are 98.57%, 98.32% and 94.38% for the red, blue and green lines respectively.

ACKNOWLEDGMENTS

R.X.W. is supported by China Postdoctoral Science Foundation (2016M600999). Z.Q.Y. is supported by National Natural Science Foundation of China (NSFC) (61435007 and 61771278), and Joint Fund of the Ministry of Education of the People's Republic of China (MOE)

(6141A02011604). G.L.L is supported by National Natural Science Foundation of China (NSFC) (20141300566).

-
- [1] L. M. Duan, M. D. Lukin, I. Cirac, P. Zoller, *Nature* **414**, 413 (2001).
- [2] Z. Q. Yin and F. L. Li, *Phys. Rev. A* **75**, **012324** (2007).
- [3] Chao Song, et al, arXiv:1703.10302.
- [4] Q. Hou, W. Yang, C. Chen and Z. Yin, *J. Opt. Soc. Am. B* **33**, 2242 (2016).
- [5] X. Wang, A. Miranowicz, H. R. Li, F. Nori, *Phys. Rev. A* **93**, 063861 (2016).
- [6] V. M. Stojanovic, M. Vanevic, E. Demler, and L. Tian, *Phys. Rev. B* **89**, 144508 (2014).
- [7] A. D. O'Connell, M. Hofheinz, M. Ansmann, et al., *Nature*, **464**, 7289 (2010).
- [8] M. J. A. Schuetz, E. M. Kessler, G. Giedke, L. M. K. Vandersypen, M. D. Lukin, and J. I. Cirac, *Phys. Rev. X* **5**, 031031 (2015).
- [9] P. Arrangoiz-Arriola and A. H. Safavi-Naeini, *Phys. Rev. A* **94**, 063864 (2016).
- [10] M. V. Gustafsson, T. Aref, A. F. Kockum, M. K. Ekström, G. Johansson, and P. Delsing, *science* **346**, 6206 (2014).
- [11] S. M. Meenehan, J. D. Cohen, G. S. MacCabe, F. Marsili, M. D. Shaw, and O. Painter, *Phys. Rev. X* **5**, 041002 (2015).
- [12] R. Manenti, A. F. Kockum, A. Patterson, T. Behrle, J. Rahamim, G. Tancredi, F. Nori, and P. J. Leek, arXiv:1703.04495.
- [13] C. Galland, N. Sangouard, N. Piro, N. Gisin, and T. J. Kippenberg, *Phys. Rev. Lett.* **112**, 143602 (2014).
- [14] O. Matsuda, O. B. Wright, D. H. Hurley, V. Gusev, K. Shimizu, *Phys. Rev. B* **77**, 224110 (2008).
- [15] O. Matsuda, O. B. Wright, D. H. Hurley, V. E. Gusev, and K. Shimizu, *Phys. Rev. Lett.* **93**, 095501 (2004).
- [16] Y. Yanay and A. A. Clerk, *New J. Phys.* **19**, 033014 (2017).
- [17] J. H. Chai, Y. Q. Lu, *Physica B* **291**, 292 (2000).
- [18] X. Baia, T. A. Eckhausea, S. Chakrabartib, P. Bhattacharyab, R. Merlina, C. Kurdak, *Physica E* **34**, 592 (2006).
- [19] M. J. Woolley, A. C. Doherty, and G. J. Milburn, *Phys. Rev. B* **82**, 094511 (2010).
- [20] C. Ohm, C. Stampfer, J. Splettstoesser, and M. R. Wegewijs, *Appl. Phys. Lett.* **100**, 143103 (2012).
- [21] O. P. deSaNeto, M. C. deOliveira, F. Nicacio, and G. J. Milburn, *Phys. Rev. A* **90**, 023843 (2014).
- [22] S. Gleyzes, S. Kuhr, C. Guerlin, J. Bernu, S. Deléglise, U. B. Hoff, M. Brune, J. M. Raimond and S. Haroche, *nature* **446**, 05589 (2007).
- [23] M. Eichenfield, J. Chan, R. M. Camacho, K. J. Vahala, and O. Painter, *Nature* **462**, 78 (2009).
- [24] P. Ouartchaiyapong, K. W. Lee, B. A. Myers, and A. C. B. Jayich, *Nat. Comm.* **5**, 4429 (2014).
- [25] D. A. Golter, T. Oo, M. Amezcua, K. A. Stewart, and H. Wang, *Phys. Rev. Lett.* **116**, 143602 (2016).
- [26] E. R. MacQuarrie, M. Otten, S. K. Gray, and G. D. Fuchs, *Nat. Comm.* **8**, 14358 (2017).
- [27] P. Rabl, P. Cappellaro, M. V. G. Dutt, L. Jiang, J. R. Maze, and M. D. Lukin, *Phys. Rev.* **79**, 041302 (2008).
- [28] P. Rabl, S. J. Kolkowitz, F. H. L. Koppens, J. G. E. Harris, P. Zoller, and M. D. Lukin, *Nat. Phys.* **6**, 602 (2010).
- [29] Z. Y. Xu, Y. M. Hu, W. L. Yang, M. Feng and J. F. Du, *Phys. Rev. A* **80**, 022335 (2009).
- [30] L. G. Zhou, L. F. Wei, M. Gao, and X. B. Wang, *Phys. Rev. A* **81**, 042323 (2010).
- [31] Z. Q. Yin, T. C. Li, X. Zhang, and L. M. Duan, *Phys. Rev. A* **88**, 033614 (2013).
- [32] Y. Ma, Z. Q. Yin, P. Huang, W. L. Yang, and J. F. Du, *Phys. Rev. A* **94**, 053836 (2016).
- [33] K. Cai, R. X. Wang, Z. Q. Yin, G. L. Long, *Sci. Chi.* **60**, 070311 (2017).
- [34] S. D. Bennett, N. Y. Yao, J. Otterbach, P. Zoller, P. Rabl, and M. D. Lukin, *Phys. Rev. Lett.* **110**, 156402 (2013).
- [35] D. A. Golter, T. Oo, M. Amezcua, I. Lekavicius, K. A. Stewart, and H. Wang, *Phys. Rev. X* **6**, 041060 (2016).
- [36] D. A. Golter, T. Oo, M. Amezcua, K. A. Stewart, and H. Wang, *Phys. Rev. Lett.* **116**, 143602 (2016).
- [37] J.R. Maze, A. Gali, E. Togan, Y. Chu, A. Trifonov, E. Kaxiras, and M. D. Lukin, *New J. Phys.* **13**, 025025 (2011).
- [38] M. W. Doherty, N. B. Manson, P. Delaney, and L. C. L. Hollenberg, *New J. Phys.* **13**, 025019 (2011).
- [39] V. B. Braginsky, and F. Y. Khalili, *Quantum Measurement* (ed. Thorne, K. S.) Chs IV and XI (Cambridge Univ. Press, Cambridge, UK, 1992).
- [40] P. Grangier, J. A. Levenson, and J. P. Poizat, *Nature* **396**, 537 (1998).
- [41] G. Nogues, et al., *Nature* **400**, 239 (1999).
- [42] N. B. Manson, J. P. Harrison, and M. J. Sellars, *Phys. Rev. B* **74**, 104303 (2006).
- [43] S. Saito, X. Zhu, R. Amsüss, Y. Matsuzaki, K. Kakuyanagi, T. Shimo-Oka, N. Mizuochi, K. Nemoto, W. J. Munro, and K. Semba, *Phys. Rev. Lett.* **111**, 107008 (2013).
- [44] L. J. Rogers, S. Armstrong, M. J. Sellars and N. B. Manson, *New J. Phys.*, **10**, 103024 (2008).
- [45] Zhang-qi Yin, Zhao Nan, Tongcang Li, *Science China Physics, Mechanics & Astronomy* **58**, 050303 (2015).
- [46] L. M. Duan, A. Kuzmich, and H. J. Kimble, *Phys. Rev. A* **67**, 032305 (2003).
- [47] Zhang-qi Yin, W. L. Yang, Luyan Sun, L. M. Duan *Phys. Rev. A* **91**, 012333 (2015).
- [48] J. I. Cirac, P. Zoller, H. J. Kimble, and H. Mabuchi, *Phys. Rev. Lett.* **78**, 3221 (1997).
- [49] D. F. V. James and J., *Canadian Journal of Physics*, **6**, 625 (2007).
- [50] L. Robledo, H. Bernien, V. D. S. Toeno, R. Hanson, *New J. Phys.* **13**, 119 (2010).
- [51] N. Bar-Gill, L.M. Pham, A. Jarmola, D. Budker, and R.L. Walsworth, *Nat. Commun.* **4**, 1743 (2013).
- [52] Y. Tao, J. M. Boss, B. A. Moores, and C. L. Degen, *Nat. Commun.* **5**, 3638 (2014).